Desalination and Water Treatment
www.deswater.com
doi: 10.1080/19443994.2014.970579

57 (2016) 845–860
January

Taylor & Francis
Taylor & Francis Group

Adsorption and desorption of phenol onto barley husk-activated carbon in an airlift reactor

Margarita Loredo-Cancino, Eduardo Soto-Regalado*, Refugio Bernardo García-Reyes, Felipe de Jesús Cerino-Córdova, María Teresa Garza-González, Mónica María Alcalá-Rodríguez, Nancy Elizabeth Dávila-Guzmán

Facultad de Ciencias Químicas, Universidad Autónoma de Nuevo León, UANL, Av. Universidad S/N, Ciudad Universitaria, San Nicolás de los Garza, NL 66451, Mexico, Tel./Fax: +52 8183294000, ext. 6290; email: margarita.loredo@gmail.com (M. Loredo-Cancino), Tel./Fax: +52 8183294000; email: edsoto1962@yahoo.com.mx (E. Soto-Regalado), Tel./Fax: +52 8183294000, ext. 6288; email: bernardogarciareyes@yahoo.com.mx (R.B. García-Reyes), Tel./Fax: +52 8183294000, ext. 6281; email: felipejccuanl@yahoo.com.mx (F.J. Cerino-Córdova), Tel./Fax: +52 8183294000; emails: mteresaggzz@yahoo.com (M.T. Garza-González), labiquanl@hotmail.com (M.M. Alcalá-Rodríguez), Tel./Fax: +52 8183294000, ext. 6282; email: nancydavilagz@gmail.com (N.E. Dávila-Guzmán)

Received 13 March 2014; Accepted 23 September 2014

ABSTRACT

Batch studies of phenol adsorption onto barley husk-activated carbon (BHAC) were performed at different BHAC doses, solution pH, temperatures, stirring speeds, BHAC particle sizes and initial phenol concentrations. The maximum phenol adsorption capacity onto BHAC was 98.83 mg g^{-1} at 25°C and pH 7, similar to commercial activated carbon. The external mass transfer was minimised at stirring speeds greater than 400 min^{-1}, and the adsorption kinetics were affected by both the initial phenol concentration and the temperature. Ethanol/water solutions at 10% V/V were the most effective regenerating agent, with a desorption capacity of 47.79 mg g^{-1}, after five adsorption–desorption cycles. The breakthrough data for phenol adsorption using an airlift reactor were obtained at different air flow rates, initial phenol concentrations, BHAC doses and influent flow rates. Experimental data confirmed that the time to achieve the breakthrough point increases when the air flow rate or the BHAC dosage increases, as a result of more turbulent flow or greater available surface area, respectively. Additionally, the breakthrough point decreases when the initial phenol concentration or inlet flow rate increases, due to the rapid exhaustion of adsorption sites. These promising results demonstrate the feasibility of adsorption in continuous operation in an airlift reactor.

Keywords: Airlift reactor; Breakthrough curves; Desorption; Intraparticle diffusion; Modelling

1. Introduction

Phenol (C_6H_6O) is a common pollutant present in the wastewaters of industries, such as refineries, coal processors, olive mills, and the manufacturers of petrochemicals, fabrics, plastics, wood products, paints, papers and resins, among others. Phenol may have harmful effects on both public health and aquatic life; for example, it has been found that the metabolism,

*Corresponding author.

survival, growth and reproductive system of fish are affected when they live in phenolic-polluted water [1]. In humans, the effects of repeated oral exposure to phenol include diarrhoea, mouth sores and dark urine [2]. Furthermore, the ingestion of 1 g of phenol is fatal [3]. Consequently, the treatment of phenol-containing wastewater is required prior to its discharge.

Adsorption onto activated carbon is widely recognised as one of the most efficient methods for phenol removal at low concentrations from wastewater. However, the use of commercial activated carbon as adsorbents is often limited due to economic reasons; thus, the use of low-cost precursors, such as agro-waste materials, for the production of activated carbon and its use on phenol removal from aqueous solutions have been investigated in several studies [4–12]. In México, the INEGI reported that 8.2×10^6 L of beer were produced in 2008 [13]. This industrial activity generated large quantities of barley husk as a by-product, and this waste was previously used as a precursor for the activated carbon [14]. This material was used as an adsorbent in this research due to its physicochemical properties, which includes high surface area and surface functional groups.

In addition to the high cost, the main drawback of the use of activated carbon as an adsorbent is the secondary pollution generated by the disposal of the spent adsorbent. To overcome this disadvantage, there are numerous adsorbent regeneration techniques used to re-establish the maximum adsorbent capacity and to preserve, as much as possible, the initial weight and pore structure of the adsorbent. Thermal regeneration is one of the desorption methods most widely employed. In this method, the adsorbates are desorbed by means of volatilisation and oxidation at high temperature. However, this method has disadvantages, such as the loss of activated carbon by attrition (5–10%), due to excessive burn off and washout during each cycle [15]. Chemical regeneration of adsorbents is a feasible alternative because it has some advantages; for instance, it can be performed in situ, there are no losses of activated carbon (unlike in thermal desorption), it is possible to recover valuable adsorbates and the chemical reagents can be reused [16].

Commonly, the process of adsorption in the liquid phase has been carried out mostly in the fixed-bed columns in a continuous flow operation. Nevertheless, the operational complexity and the limitation of the removal efficiency have led to a search of new and efficient equipment that can provide better removal efficiency without additional mechanical complications. Airlift reactors have drawn increased attention as possible alternatives to fixed-bed columns because of their advantages such as a simple construction without moving parts, a high liquid phase content, a low operational shear stress and good mixing properties with minimal energy consumption [17]. Additionally, airlift reactors allow the use of powdered adsorbents, which is not possible in fixed-bed columns due to high pressure drops, and the use of adsorbents with low hardness values, due to the low shear stress in the reactor. Therefore, the objective of this study is to investigate the effect of a number of variables on the batch, and continuous operations (of an airlift reactor) of phenol adsorption onto barley husk-activated carbon (BHAC) and the regeneration of the adsorbent with four different eluents.

2. Materials and methods

2.1. Adsorbents

The BHAC used in this study was produced according to the procedure described by Loredo–Cancino et al. [14] and the CAC was purchased from Jalmek (México). Prior to adsorption experiments, both BHAC and CAC were ground to obtain particles in the range of 0.074–0.150 mm. The main characteristics of BHAC and CAC are discussed in Section 3.

2.2. Adsorbate

A stock solution of 1,000 mg L^{-1} was prepared with phenol (Sigma–Aldrich, purity ≥ 99%). Appropriate dilutions were performed to obtain initial phenol concentrations ranging from 50 to 1,000 mg L^{-1} and these solutions were used in the adsorption experiments. Phenol solutions were prepared using distilled water. The initial and final phenol concentrations were measured with a UV spectrophotometer (Varian Cary 50) at a wavelength of 290 nm.

2.3. Materials characterisation

The surface characterisation of CAC was carried out using an ASAP 2020 (Micromeritics) analyser. The adsorbent was out-gassed at 500 μm Hg and 100˚C for 360 min. Adsorption isotherms were generated by dosing nitrogen (99.999% purity), and data were recorded. Pore size distribution and specific surface area were calculated using the BET equation, and the total pore volume was obtained from the amount of nitrogen adsorbed at the relative pressure of 0.98.

It is well known that the adsorption can be strongly affected by the nature and quantity of surface oxygenate groups. The surface acidity studies were determined based on the method reported by Al-Degs et al. [18]. Samples (0.5 g) of BHAC and CAC were

shaken in 50 mL of 0.01 M NaOH for 24 h at room temperature. Thereafter, the samples were filtered and the remaining NaOH was titrated with 0.01 M HCl. These experiments were conducted in triplicate, and the results are expressed in meq of H^+ g^{-1} of the adsorbent.

2.4. Equilibrium adsorption experiments

To determine an appropriate adsorbent dosage to be used in equilibrium adsorption experiments, a known mass of BHAC (0.02–0.25 g) was added to flasks of 50 mL containing 25 mL of 500 mg L^{-1} phenol solution, and stirred using an orbital shaker with a temperature controller (Barnstead MAX Q 4000) at 200 min^{-1} and 25°C. Once the adsorbent dosage was determined in the previous experiment, the equilibrium adsorption experiments were conducted with varying phenol concentrations from 50 to 1,000 mg L^{-1} and temperatures of 25, 35 and 45°C, using 50-mL flasks containing 25 mL of the phenol solution. These flasks were continuously stirred using an orbital shaker with a temperature controller at 200 min^{-1} until equilibrium was achieved. Solution pH was adjusted, during the experiment, to the appropriate level by adding NaOH or HCl as required. The initial and final phenol concentrations were measured with a UV–vis spectrophotometer. All experiments were conducted in triplicates. The quantity of phenol adsorbed onto the activated carbon (q) and the removal percentage (R) of phenol were calculated according to Eqs. (1) and (2), respectively.

$$q = \frac{V(C_0 - C)}{W} \tag{1}$$

$$R = \frac{C_0 - C}{C_0} \times 100 \tag{2}$$

where C_0 is the initial phenol concentration, V is the volume of the solution, W is the mass of the activated carbon and C is the residual phenol concentration either at equilibrium or at any time t, which defines q_e or q_t, respectively.

2.5. Adsorption kinetic experiments

A rotating-basket reactor [19,20] was used for kinetic experiments. This basket contained the adsorbent, and it was submerged in a beaker containing the phenol solutions. It is important to note that the rotating basket reactor was equipped with six equally spaced baffles to prevent vortex formation and a propeller stirrer for complete mixing. The beaker was partially immersed in a water bath to keep the temperature of the phenol solution constant. A known mass of BHAC (0.8 g) was placed in the basket and the basket was attached to the shaft of the stirrer. A 1,000 mL solution of a known initial concentration of phenol (250, 500 or 1,000 mg L^{-1}) was poured into the beaker; the pH of the solution was kept at 7. Afterwards, the basket was immersed in the beaker, and the timer and the motor of the stirrer were simultaneously activated. Once the experiments were started, the contents were mixed at a set stirring speed (300, 400 or 500 min^{-1}). Samples of the solution were withdrawn at selected intervals of time, and the adsorption capacity at time t was calculated with Eq. (1), taking into account the withdrawn sample volume.

2.6. Regeneration of spent activated carbon

Distilled water, 0.1 N HCl, 0.1 N NaOH and 10% V/V ethanol/water were used as the regenerating agents. Samples of 0.02 g of activated carbon were added to 25 mL of phenol solutions containing 1,000 mg L^{-1} at 30°C. These experiments were continuously stirred at 200 min^{-1}, and the solution pH was adjusted to 7 until the equilibrium was achieved. Adsorption capacity at equilibrium was calculated with Eq. (1). The adsorbent was separated from phenol solutions by filtration, and phenol was desorbed from the phenol-loaded activated carbon with 25 mL of the tested eluents at 30°C for 4 h at 200 min^{-1}. The regenerated activated carbon was separated by filtration and was used for adsorption of phenol at the same condition as described above.

2.7. Airlift reactor adsorption studies

The dynamic adsorption of phenol onto BHAC was performed in a stainless steel airlift reactor from Applikon Biotechnology (The Netherlands). The reactor consisted of a vertical cylindrical stainless steel column of 5-cm diameter and 38-cm length, fitted concentrically into another vertical cylindrical stainless steel column of 6-cm diameter and 60-cm length, as shown in Fig. 1. The temperature of the airlift reactor was monitored with a temperature sensor located at the bottom of the reactor and maintained at 30°C with a heating blanket. The airlift reactor was loaded with 6 or 15 g of BHAC. Two Masterflex peristaltic pumps enabled synthetic phenolic wastewater to flow through the airlift reactor at a flow rate of 2 or 3 L h^{-1}. The feed port was located at the bottom centre of the

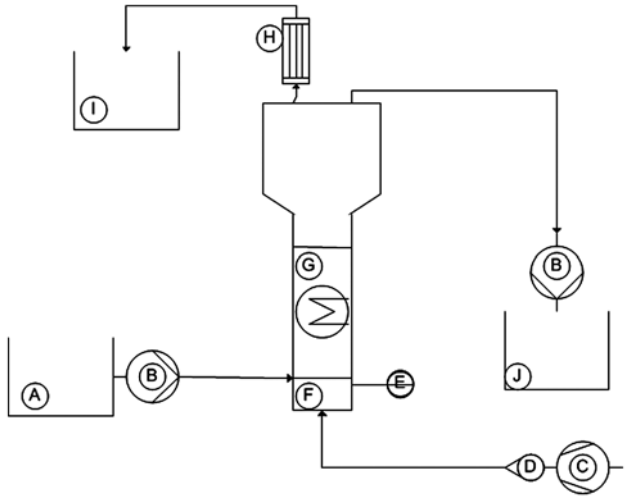

Fig. 1. Schematic representation of the airlift reactor used to conduct the dynamic adsorption of phenol onto BHAC. (A): phenolic solution reservoir; (B): peristaltic pump; (C): compressor; (D): rotameter; (E): thermometer; (F): airlift reactor; (G): heating blanket; (H): condenser; (I): condensation; (J): treated effluent.

reactor; consequently, the solution flowed upwards. The sampling port and a stainless steel air-outlet condenser were located at the top of the reactor to collect samples and prevent the loss of phenolic solutions by evaporation, respectively. Samples were collected at selected time intervals and analysed for phenol concentration using a UV–Vis spectrophotometer (Varian Cary 50) at a wavelength of 290 nm. The value of the initial phenol concentration was 40 or 250 mg L^{-1} and the overall sampling period was 516 min.

2.8. Error analysis

The average relative error (ARE) was used as an error function to determine the accuracy of the non-linear regression, which was performed to fit the selected models to the experimental data. This error function attempted to minimise the fractional error distribution across the entire studied range. The model parameters were determined using the Solver® function of Microsoft Excel, and the ARE was minimised according to Eq. (3):

$$\mathrm{ARE} = \left(\frac{1}{N}\sum_{i=1}^{N}\left|\frac{q_{\mathrm{exp}} - q_{\mathrm{calc}}}{q_{\mathrm{exp}}}\right|\right) \times 100 \quad (3)$$

where N is the number of experimental points, and q_{exp} and q_{calc} represent the experimental and predicted phenol concentrations, respectively.

3. Results and discussion

Adsorption experiments on BHAC and CAC were carried out by varying the concentrations of adsorbent and adsorbate, pH, temperature, stirring speed and mean particle size. The effect of these variables on the adsorption of phenol from aqueous solution is discussed in the following sections.

3.1. Effect of adsorbent dose

Fig. 2 shows the effect of BHAC dose on the adsorption capacity and the removal of phenol. The removal of phenol increased from 10 to 75% when the BHAC dose increased from 0.8 to 10 g L^{-1}. The increased adsorbent dose resulted in more available sites to adsorb phenol from aqueous solutions. However, phenol adsorption capacity decreased from 70 to 35 mg g^{-1} because not all available sites for the adsorbate were occupied at the high adsorbent dose. Thus, a BHAC dosage of 0.8 g L^{-1} was used for further studies.

3.2. Effect of pH

The adsorption of phenols from aqueous solution is a result of the combined effects of pH on the ionisation of phenol, inorganic acids and bases present (used to adjust pH), and the adsorbent surface charge distribution [11]. Fig. 3 depicts the effect of pH on the adsorption capacity of phenol. For a range of 3–11, the effect of pH was studied at 0.8 g BHAC L^{-1}, a contact time of 24 h, a stirring speed of 200 min^{-1}, an initial phenol concentration of 500 mg L^{-1} and a temperature of 25°C. The adsorption capacity of phenol onto BHAC increased when the pH was increased from 3 to 7. At pH 7, the highest adsorption capacity of phenol onto BHAC was achieved and it decreased as the pH increased to 11. This behaviour can be explained in terms of the dissociation constant of phenol (pK_a = 9.89) and the pH of the point of zero charge (pH_{PZC} = 1.9) of BHAC (Table 1). At a solution pH higher than the pK_a value of phenol, the adsorbate is primarily present in the aqueous phase as phenolate (i.e. a negatively charged species), and according to the BHAC pH_{PZC} value, the BHAC net surface charge is predominantly negative. Therefore, the electrostatic repulsive forces between the phenolate and the negative surface of carbon may decrease the phenol adsorption capacity at pH values greater than 9.89. The observed reduction in phenol adsorption capacity at pH values below 7 suggests that additional protons added in the phenol solution to obtain the pH values of 3, 4 and 5 compete with phenol for carbonyl oxygen

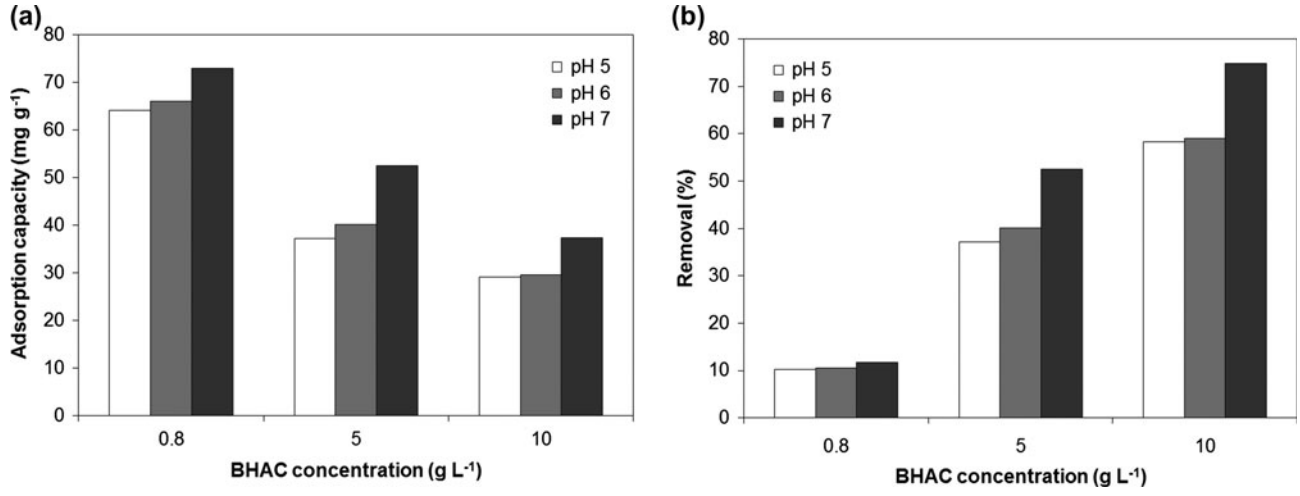

Fig. 2. The effect of the BHAC dose on (a) the adsorption capacity (q_e, mg g^{-1}) and (b) phenol removal efficiency (%) at initial phenol concentration of 500 mg L^{-1} and 30˚C.

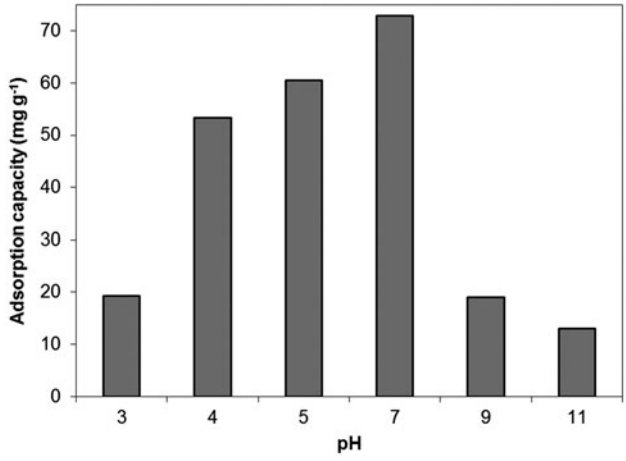

Fig. 3. The effect of pH on the phenol adsorption capacity onto BHAC (q_e, mg g^{-1}) at initial phenol concentration of 500 mg L^{-1} and 30˚C.

Table 1
Physicochemical properties of BHAC and CAC [14]

Parameter	BHAC	CAC
pH_{PZC}*	1.9	4.2
Total surface acid sites (meq g^{-1})*	2.4	1.6
BET surface area (m^2 g^{-1})	810	1,350
Total pore volume (cm^3 g^{-1})	0.4	1.0
Average pore width (nm)	2.6	3.1

*Precision of replicate samples averaged 5%.

sites, where the adsorption occurs by an electron donor–acceptor complex formation at the carbon surface. Surface structural characteristics determined by the infrared internal reflection spectroscopy presented by Mattson et al. [21] suggested that the electron donor–acceptor complex was formed between the oxygen of the surface carbonyl group (electron donor) and the phenol aromatic ring (electron acceptor).

3.3. Equilibrium adsorption experiments

As expected, the temperature of wastewater changes with the environmental conditions, the plant production capacity or as a result of unexpected events. Therefore, knowledge of the adsorption equilibrium at different temperatures is an important factor in the design of adsorption systems. For example, to design batch adsorption systems, the parameters of different adsorption isotherms are required to determine the masses of adsorbents for each specific application.

A number of equilibrium isotherm models have been formulated, but the Langmuir [22], Freundlich [23] and Sips [24] isotherms are the most frequently used. However, as is the case for all models, there are equation limitations that need to be tested. As such, the aforementioned isotherm models were compared. Their expressions are given in Eq. (4) (Langmuir), Eq. (5) (Freundlich), and Eq. (6) (Sips), and the resultant parameters after the application to the experimental adsorption data are provided in Table 2.

$$q_e = \frac{q_m b C_e}{1 + b C_e} \tag{4}$$

$$q_e = K C_e^{1/n} \tag{5}$$

Table 2
Isotherm parameters estimated from experimental data of phenol adsorption onto BHAC at pH 7

Temperature (°C)	Langmuir			Freundlich			Sips			
	q_m	b ($\times 10^3$)	ARE (%)	K	$1/n$	ARE (%)	q_m	a ($\times 10^3$)	n	ARE (%)
25	132.9	2.1	11.1	2.7	0.5	2.4	127.7	43.9	0.4	18.4
35	95.9	2.4	5.1	1.8	0.5	2.4	158.9	4.3	0.8	5.6
45	125.6	1.5	8.0	0.7	0.7	11.4	141.4	1.7	1.0	9.6

$$q_e = \frac{q_m a C_e^n}{1 + a C_e^n} \tag{6}$$

The equilibrium isotherms of phenol on BHAC at pH 7, temperatures of 25, 35 and 45°C and phenol concentrations from 50 to 1,000 mg L^{-1} are presented in Fig. 4(a). The maximum experimental adsorption capacity of phenol onto BHAC increased from 75.28 to 98.83 mg g^{-1} when the temperature decreased from 45 to 25°C (Fig. 4(a)); this increase could be related to a decrease in the vibrational energy of the adsorbed molecules, which results in less desorption of phenol from the BHAC surface [25]. The maximum experimental adsorption capacity value determined for phenol onto BHAC is similar to or higher than those reported for activated carbon produced from other lignocellulosic precursors (Table 3).

The equilibrium adsorption data of phenol onto BHAC at 25 and 35°C were satisfactorily predicted with the Freundlich isotherm. At 45°C, the experimental data were well predicted by the Langmuir model (Table 2). According to the isotherm at 25°C shown in Fig. 4(a), there was no plateau in the studied range, which could suggest that the phenol is either adsorbed in multiple layers onto BHAC, as proposed in the Freundlich isotherm or that the experiments were conducted in the linear region of the Langmuir isotherm. Additionally, the Freundlich isotherm implied that the energy distribution for the adsorption sites was an exponential type. This assumption suggests the possibility of a non-linear energy distribution for the adsorption sites of BHAC, which is consistent with a heterogeneous activated carbon surface, (consisting of basal planes and edges of microcrystallites) produced from lignocellulosic materials [26].

As observed in Fig. 4(a), an increase in temperature reduces the adsorption capacity of phenol onto BHAC. This behaviour could be explained as follows: the adsorbed phenol molecules have vibrational energies at 35 and 45°C that are greater than the energy at 25°C; therefore, these are more likely to desorb from the BHAC surface, especially to those adsorbed on the

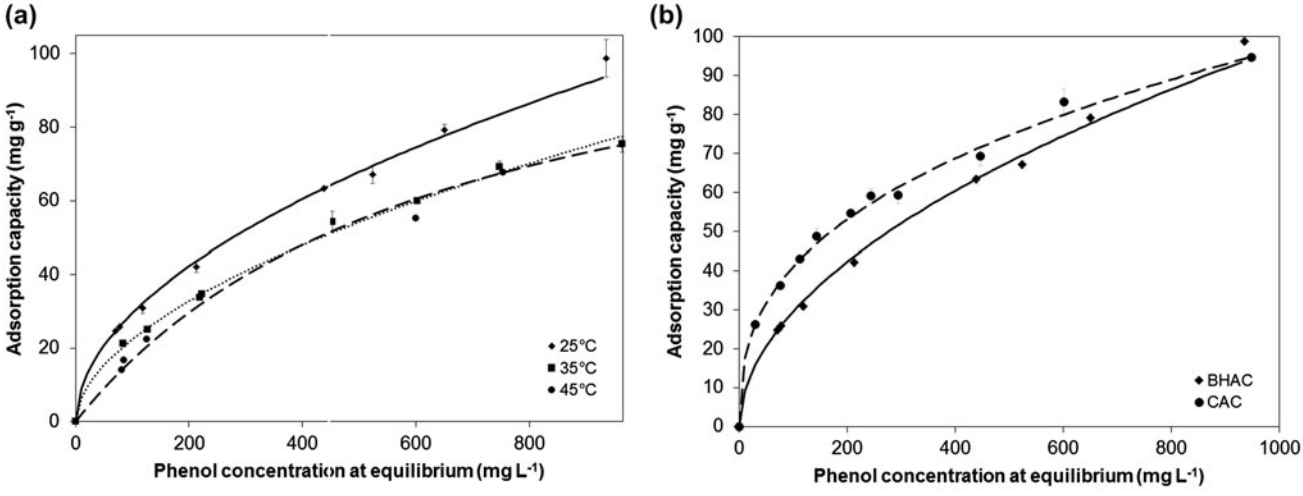

Fig. 4. (a) The adsorption isotherms of phenol onto BHAC at pH 7 and 25, 35 and 45°C. Symbols represent the experimental data and the lines indicate the Freundlich model for 25 and 35°C, and Langmuir model for 45°C and (b) the adsorption isotherms of phenol onto BHAC and CAC at pH 7 and 25°C. Symbols represent the experimental data and the lines indicate the Freundlich model prediction.

Table 3
Comparison of the BHAC characteristics with other activated carbons

Activated carbon	Surface area ($m^2\ g^{-1}$)	Phenol initial concentration ($mg\ L^{-1}$)	Adsorption capacity ($mg\ g^{-1}$)	Reference
Pecan shells AC	–	35	18	[9]
Rice husk AC	438.9	300	22.09	[5]
CAC2 (commercial, from Norit	620	100	73	[47]
Kenaf AC	1,021	188	80	[12]
Coffee residue AC	520	170	84.02	[6]
This research	810	1,000	98.83	
CAC1 (commercial, from Norit	1,350	100	104	[47]
Black gram husk AC	–	100	109.92	[10]
Vetiver roots AC	1,170	100	122	[4]
Black stone cherries AC	–	500	133.33	[8]

external layers, which results in a lower phenol adsorption capacity.

Fig. 4(b) shows the phenol adsorption isotherm onto CAC and BHAC at 25°C. It can be observed that the quantity of phenol adsorbed onto CAC is greater than that adsorbed by BHAC at equilibrium phenol concentrations below 950 $mg\ L^{-1}$. However, the adsorption data for both CAC and BHAC converge at equilibrium concentrations above 950 $mg\ L^{-1}$. The difference between the adsorption capacities of BHAC and CAC could be explained on the basis of different surface areas and total surface acidic sites. The BHAC used in this research had a surface area of 810 $m^2\ g^{-1}$ and 2.4 meq $H^+\ g^{-1}$, whereas those of the CAC were 1,350 $m^2\ g^{-1}$ and 1.55 meq $H^+\ g^{-1}$ (Table 1). Based on the surface area, the adsorption capacity of CAC was expected to be greater than that of the BHAC as evidenced in the low equilibrium concentration regime ($C_e < 950\ mg\ L^{-1}$) as shown in Fig. 4(b). Moreover, it is proposed that the observed decrease in the adsorption capacity at low concentration is also related to water adsorption, as proposed by Coughlin and Ezra [27] and other researchers [21,28–31]. As water comes in contact with the adsorbent surface, it adsorbs on the acidic sites located at the entrance of the carbon pores, thereby reducing the accessibility of the phenol molecules to the inner pore structure. Consequently, a high surface acidic site content in BHAC leads to a lower phenol adsorption capacity because the number of sites for H-bonding is increased, and it is to be expected that adsorption of water molecules on these groups is higher than the adsorption of phenol molecules. Nonetheless, at high equilibrium concentrations of phenol ($C_e > 950\ mg\ L^{-1}$), the effects of surface area and total acidic sites diminish.

3.4. Kinetic adsorption experiments

The study of batch adsorption kinetics is relevant to the design of continuous adsorption systems. The solute uptake rate determined from the kinetic analysis determines the residence time to achieve equilibrium in an adsorption process, and it is useful for planning the scale up of adsorption equipment.

Several mathematical models have been proposed to describe the adsorption data and can be classified as the adsorption diffusion models or the adsorption reaction models. Adsorption reaction models are based on the whole process of adsorption without considering mass transfer. Adsorption diffusion models are based on a variety of steps related to mass transfer. The results and discussion of the adsorption reaction models [32,33] and adsorption intraparticle diffusion models [34,35] are presented in the subsequent sections.

3.4.1. Adsorption reaction models

The pseudo-first-order kinetic equation [32] is given by Eq. (7):

$$q_t = q_e\left(1 - e^{kt}\right) \tag{7}$$

where q_t is the amount of adsorbate adsorbed at time t, q_e is its value at equilibrium and k_1 is a constant. The pseudo-second-order kinetic equation [33] can be expressed as follows:

$$q_t = \frac{q_e^2 k_2 t}{1 + q_e k_2 t} \tag{8}$$

where k_2 is a constant.

Table 4
Comparison of the pseudo-first and pseudo-second-order kinetic models for the phenol adsorption onto BHAC at different experimental conditions

				Pseudo-first order			Pseudo-second order		
Stirring speed (min^{-1})	Mean particle diameter (mm)	C_0 (mg L^{-1})	Temperature (°C)	k_1 (min^{-1})	q_e (mg g^{-1})	ARE (%)	k_2 ($\times 10^3$, g mg^{-1} min^{-1})	q_e (mg g^{-1})	ARE (%)
300	0.4	1,000	25	0.04	75.76	7.68	0.49	84.57	5.31
400	0.4	1,000	25	0.12	79.34	1.94	1.59	88.11	6.51
500	0.4	1,000	25	0.18	77.10	2.39	3.03	83.20	3.67
400	0.1	1,000	25	0.13	78.75	3.37	1.94	87.62	3.90
400	0.4	500	25	0.09	49.74	3.06	2.02	56.13	3.73
400	0.4	250	25	0.08	38.25	3.12	3.24	40.65	6.40
400	0.4	1,000	30	0.07	80.25	4.53	0.91	89.88	2.78

Both the pseudo-first- and pseudo-second-order reaction models were used to predict the adsorption kinetics of phenol onto BHAC. Table 4 shows the adsorption rate constants, equilibrium adsorption capacities and the ARE of these models. Based on the ARE, the pseudo-first-order reaction model (ARE ≤ 5.16%) predicted the experimental results better than the pseudo-second-order reaction model (ARE ≤ 8.25%) for all conditions except for experiments carried out at 300 min^{-1} and at 30°C . Few satisfactory fits of kinetic experimental data with pseudo-first-order model have been reported [17,36,37].

Fig. 5(a) shows the experimental results of the adsorption kinetics of phenol onto BHAC at different stirring speeds and the predicted values with the pseudo-first-order model. The phenol removal increased with time and attained equilibrium at approximately 40 min, under stirring speeds of 400 and 500 min^{-1} and at 120 and 300 min^{-1}. This behaviour is due to the decreased external mass transfer resistance at stirring speeds greater than 400 min^{-1}; therefore, phenol molecules are transferred at a faster rate to the external surface of the adsorbent. Further increase in the stirring speed was not necessary to reduce the time required to achieve equilibrium in the adsorption of phenol onto BHAC. For this reason, the subsequent adsorption kinetic experiments of phenol adsorption onto BHAC were only performed at 400 min^{-1}.

Fig. 5(b) shows the experimental adsorption capacity of phenol onto BHAC at two mean particle sizes (0.1 and 0.4 mm) and the adsorption capacity predicted by the pseudo-first-order model. The phenol equilibrium adsorption was attained at approximately 40 min in both cases; a reduction in the mean particle size did not improve the intraparticle diffusion because the external mass transfer had already been minimised at 400 min^{-1}. Therefore, the time needed to achieve equilibrium cannot be decreased for mean particle sizes below 0.1 mm.

Fig. 5(c) shows the experimental adsorption capacity of phenol onto BHAC at three initial phenol concentrations (250, 500 and 1,000 mg L^{-1}) and the adsorption capacity predicted by the pseudo-first-order model. The initial phenol concentration determines both the equilibrium concentration and the adsorption rate of phenol. The phenol removal attained equilibrium at approximately 40 min at an initial concentration of 1,000 mg L^{-1} and at 60 min at initial concentration of 500 and 250 mg L^{-1}, respectively. It was also observed that increasing the initial phenol concentration from 250 to 1,000 mg L^{-1} increased the equilibrium adsorption capacity by two-fold. The increased equilibrium adsorption capacity is related to the larger concentration gradient, which is the driving force for the mass transfer of phenol through the film and pores of adsorbent particles [7,20].

Fig. 5(d) shows the experimental adsorption capacity of phenol onto BHAC at 30 and 35°C and the adsorption capacity predicted by the pseudo-second- and pseudo-first-order model, respectively. The adsorption temperature had an effect on both the equilibrium concentration and the adsorption rate of phenol. The equilibrium adsorption capacity at 35°C was approximately 80 mg g^{-1}, whereas at 30°C, it was approximately 90 mg g^{-1} because the increase in vibrational energy of the phenol molecules can cause desorption from the BHAC surface. It was also observed that an increase in temperature from 30 to 35°C decreased the time required to attain equilibrium from 200 to 40 min, due to an increase in the diffusion

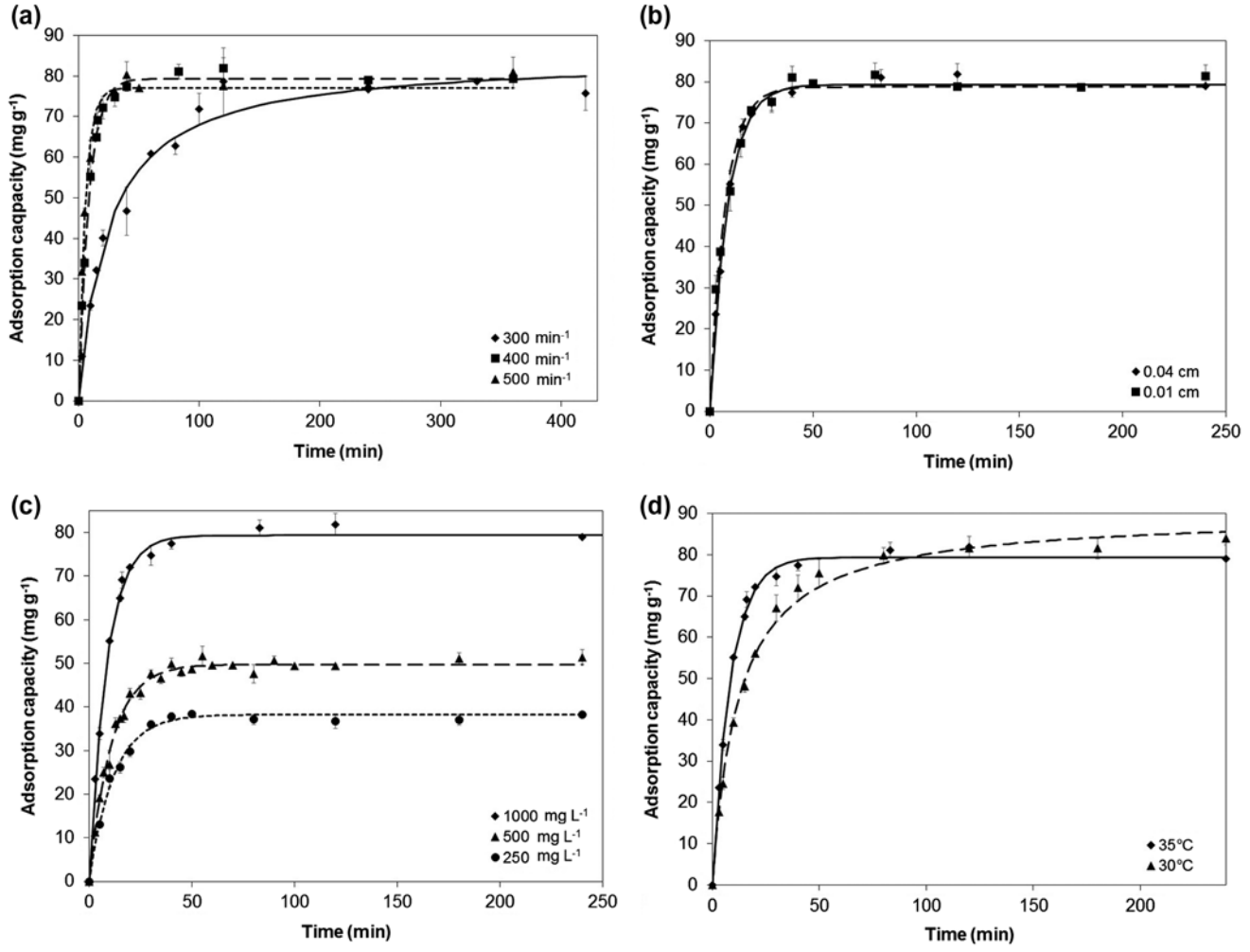

Fig. 5. Adsorption kinetics of phenol onto BHAC at pH 7, using 80 mg of BHAC in 1 L and (a) different stirring speeds, (b) different mean particle sizes, (c) different initial phenol concentrations and (d) different temperatures. Symbols represent the experimental results and the lines the predicted values by the pseudo-first-order model.

of phenol through the film and pores of adsorbent particles.

3.4.2. Adsorption intraparticle diffusion models

The simplified Vermeulen's approximation of the equation for the dimensionless fractional uptake of solute in the solid phase, q/q_∞ for adsorption on spherical particles, is provided in Eq. (9) [34]:

$$\ln\left[\frac{1}{1-F^2(t)}\right] = \frac{\pi^2 D_i t}{r_0^2} \tag{9}$$

Moreover, for small times, a plot of q/q_∞ vs. $t^{1/2}$ should result in a straight line. Because q_∞ is a constant equal to the final value of q_t, a plot of q_t alone vs. $t^{1/2}$ should also be linear. Therefore, the equation describing the Weber and Morris [34] intraparticle diffusion model is as follows:

$$q_t = k_p t^{0.5} + I \tag{10}$$

where I is the intercept that could be associated with the thickness of the boundary layer [38]. A value of I around zero indicates that diffusion is the only controlling step of the adsorption process [38]. The slope of the plot is defined as a rate parameter (k_p), which characterises the rate of adsorption, as given in Eq. (11):

$$k_p = \left(\frac{3q_e}{d_p}\right)\sqrt{\frac{D_i}{\pi}} \tag{11}$$

where d_p is the mean particle diameter from which D_i can be determined.

The phenol adsorption data were plotted according to Eq. (10) for different agitation speeds (300, 400 and 500 min^{-1}), mean particle sizes (0.01 and 0.04 cm), initial phenol concentrations (250, 500 and 1,000 mg L^{-1}) and temperatures (30 and 35°C), and the results are shown in Fig. 6. These graphics show two linear sections. The first linear section intercepts the origin, which suggests that intraparticle diffusion is the only rate-limiting step [39]. The second linear section does not intercept the origin, which implies that more than one diffusion mechanism is occurring at the same time in the adsorption process of phenol onto BHAC. Similar behaviours for adsorption process of other adsorbates have been reported in some of the previous studies [39,40]. The initial slope represents the intraparticle diffusion process according to Eq. (10), and the plateau portion corresponds to the final equilibrium process. In the first stage, the phenol diffusion is primarily restricted by the highly porous structure of the BHAC (Table 1), and during the following stage, the diffusion is predominantly retarded by the surface diffusion of phenol species along the pore surface.

Table 5 shows the parameters of the intraparticle diffusion model calculated from Eqs. (9) and (11). It can be observed that diffusivities for the first linear part of the plot and diffusivities calculated from Eqs. (9) and (11) are at 10^{-12} m^2 s^{-1} orders of magnitude, which are lower than the diffusivities of the liquid phase at ordinary temperatures [41] and can be related to BHAC porosity and the tortuosity factor [42].

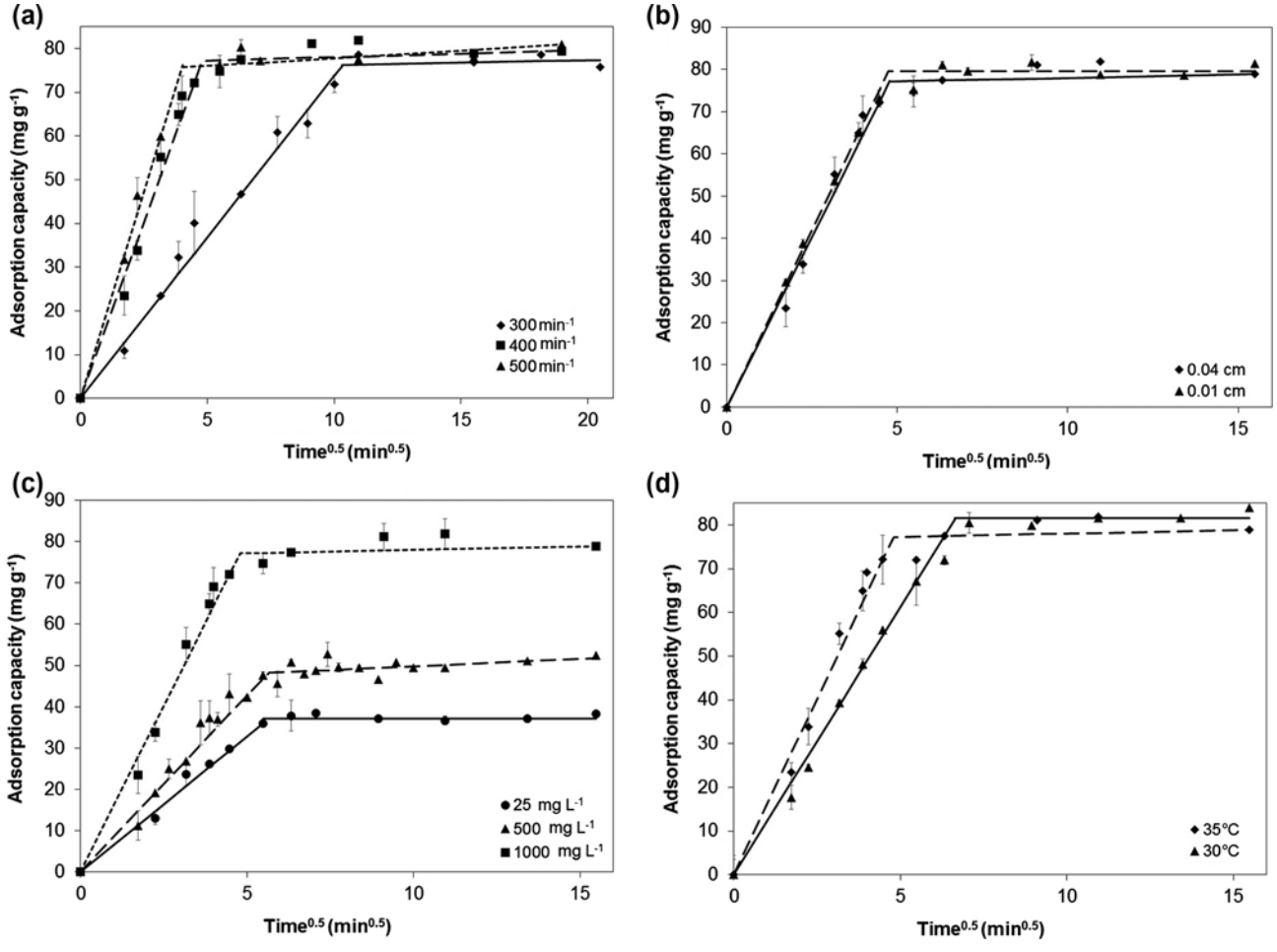

Fig. 6. Adsorption kinetics of phenol onto BHAC at pH 7, using 80 mg of BHAC in 1 L and (a) different stirring speeds, (b) different mean particle sizes, (c) different initial phenol concentrations and (d) different temperatures. Symbols represent the experimental results and the lines the predicted values by the intraparticle diffusion model.

Table 5
Fitting parameters for intraparticle diffusion model and the diffusion coefficient values for phenol adsorption onto BHAC

Stirring speed (min−1)	Mean particle diameter (mm)	C_0 (mg L^{-1})	Temperature (°C)	Weber and Morris intraparticle diffusion model								Vermeulen's approximation D_i ($\times 10^{12}$ m^2 s^{-1})
				First linear part of the curve				Second linear part of the curve				
				k_p (mg g^{-1} $min^{-0.5}$)	I (mg g^{-1})	ARE (%)	D_i ($\times 10^{12}$ m^2 s^{-1})	k_p (mg g^{-1} $min^{-0.5}$)	I (mg g^{-1})	ARE (%)	D_i ($\times 10^{14}$ m^2 s^{-1})	
300	0.4	1,000	35	7.38	0.00	7.00	5.44	0.11	75.06	1.33	0.12	3.50
400	0.4	1,000	35	16.12	0.00	7.21	32.83	0.17	76.35	2.02	0.35	30.67
500	0.4	1,000	35	18.92	0.00	3.89	47.83	0.35	74.30	1.91	1.61	39.33
400	0.1	1,000	35	16.79	0.00	5.09	3.32	0.00	79.55	1.47	0.00	1.33
400	0.4	500	35	8.55	0.00	8.67	7.33	0.37	46.14	1.99	1.34	28.00
400	0.4	250	35	6.57	0.00	6.39	4.33	0.00	37.12	1.54	0.00	7.83
400	0.4	1,000	30	12.24	0.00	6.31	14.67	0.00	81.54	2.58	0.00	11.00

3.5. Desorption studies

Fig. 7(a) shows the effect of distilled water, HCl, NaOH and ethanol solution on the desorption of phenol from BHAC. According to the results shown in Fig. 7(a), it can be observed that water is not the best eluent to desorb phenol species from BHAC, likely due to the relatively low solubility of phenol in water (8.2 g per 100 g solution) [43] and the interactions between phenol and the functional groups on the BHAC surface. The highest desorption capacity (68.79 mg g^{-1}) was obtained with 10% V/V ethanol solutions because phenol can be dissolved in pure ethanol [43]. Although it is well known that the regenerating solution pH can strongly influence desorption by changing the speciation of the adsorbate and the adsorbent surface charge distribution, when 0.1 N HCl and 0.1 N NaOH were used as eluents, desorption capacities reached 55.44 and 63.00 mg g^{-1}, respectively, which are lower than those found for 10% V/V ethanol solutions. Fig. 7(b) shows the results of five adsorption/desorption cycles of phenol on BHAC using 10% V/V ethanol solution as the regenerating agent. The adsorption capacity of phenol onto BHAC decreased from 98.33 to 73.33 mg g^{-1} from the first cycle to the fifth cycle, which indicates that the adsorption sites on the BHAC surface were occupied with non-desorbed phenol molecules that gradually saturate the adsorption sites. Additional research should be conducted using higher concentration of ethanol solutions to enhance the solubility of phenol in the regeneration solution.

3.6. Phenol adsorption in an airlift reactor

The effects of the air flow rate, initial phenol concentration, BHAC dosage and influent flow rate on phenol adsorption in an airlift reactor in continuous operation are shown in Fig. 8. The adsorption process of phenol onto BHAC gradually occurred; this can be observed from the behaviour of the breakthrough curve, which did not show a linear vertical transition between the breakpoint and the saturation point. The breakpoint occurs when the effluent phenol concentration reaches a particular concentration. The drinking water regulation of the US Environmental Protection Agency sets an oral reference dose of 2 mg L^{-1} for the lifetime consumption of phenol [44]. Therefore, an effluent phenol concentration of 2 mg L^{-1} was used to determine the breakpoint.

3.6.1. Effect of air stripping on phenol removal

The effect of air stripping on phenol removal was studied in the airlift reactor without using BHAC. The experimental study demonstrated that the maximum phenol removal achievable by air stripping was 0.05% at an air flow rate of 10 L min^{-1}. This result showed that the effect of air stripping was negligible compared with the removal of phenol by BHAC adsorption. Air stripping is not effective at low gas velocities and low phenol concentrations [17].

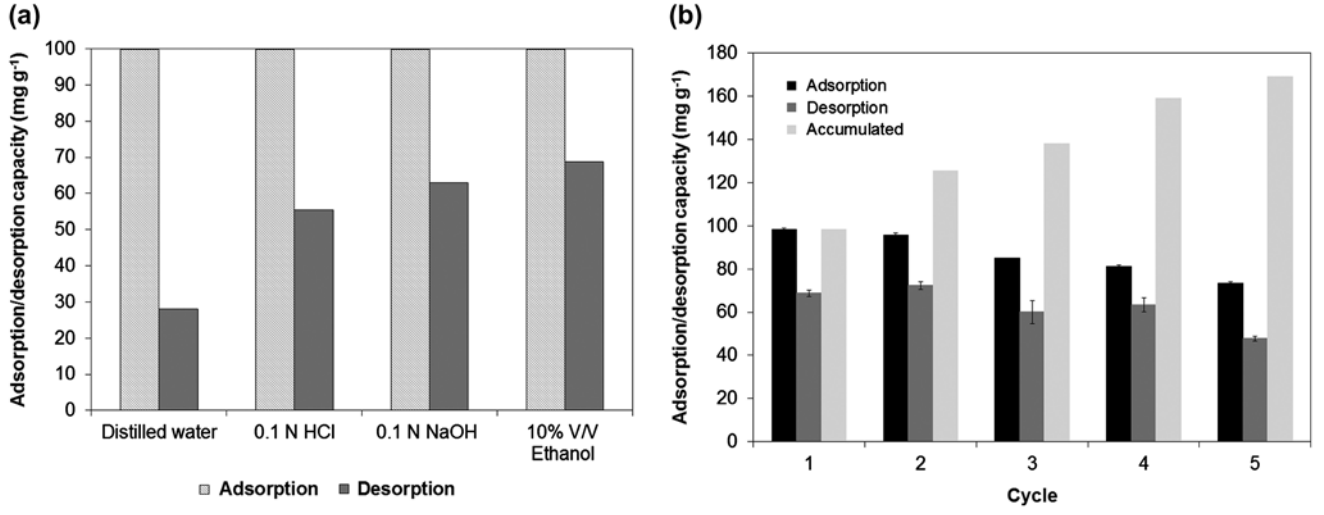

Fig. 7. (a) The effect of different regenerating agents on phenol desorption of phenol-loaded BHAC and (b) five adsorption and desorption cycles of phenol onto BHAC with 10% V/V ethanol as the regenerating agent.

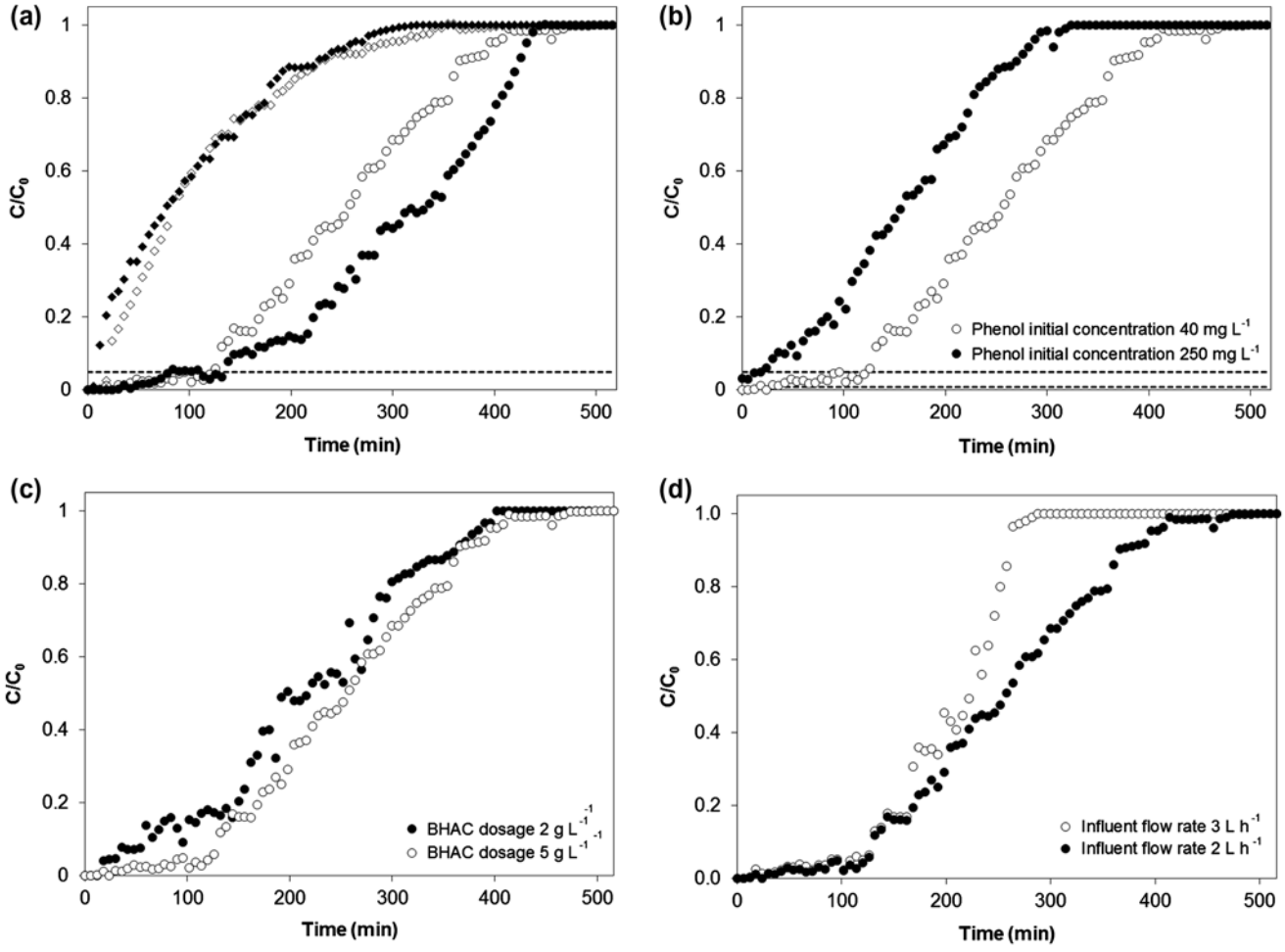

Fig. 8. (a) Effect of the air flow rate on breakthrough curves at feed concentration of 40 mg L^{-1}, (♦) BHAC dosage of 2 g L^{-1}, phenol feed rate of 3 L h^{-1}, and air flow rate of 1 L h^{-1}; (◇) BHAC dosage of 2 g L^{-1}, phenol feed rate of 3 L h^{-1}, and air flow rate of 3 L h^{-1}; (○) BHAC dosage of 5 g L^{-1}, phenol feed rate of 2 L h^{-1}, and air flow rate of 1 L h^{-1}; (●) BHAC dosage of 5 g L^{-1}, phenol feed rate of 2 L h^{-1}, and air flow rate of 10 L h^{-1}; (b) effect of phenol initial concentration on breakthrough curves at a BHAC dosage of 5 g L^{-1} and phenol feed rate of 2 L h^{-1}; (c) effect of BHAC dosage on breakthrough curves at phenol initial concentration of 40 mg L^{-1}, air flow rate of 10 L min^{-1}, and influent flow rate of 2 L h^{-1}; and (d) effect of influent flow rate on breakthrough curves at phenol initial concentration of 40 mg L^{-1}, BHAC dosage of 5 g L^{-1}, and influent Flow Rate of 2 L h^{-1}.

3.6.2. Effect of air flow rate

Fig. 8(a) shows that the time required to achieve the breakpoint increased from 12 to 18 min, when the air flow rate increased from 1 to 3 L min^{-1} at a BHAC dosage of 2 g L^{-1}. When the air flow rate increased from 1 to 10 L min^{-1} (at a BHAC dosage of 5 g L^{-1}), the breakpoint increased from 120 to 132 min. The breakthrough curve obtained at 10 L min^{-1} shows a sharper shape than the curve obtained at the lower air flow rate. At high air flow rates, the time required for a complete BHAC saturation was longer than that of lower flow rates due to a more turbulent flow that reduced the resistance of mass transfer.

3.6.3. Effect of initial phenol concentration

Fig. 8(b) shows the effect of the initial phenol concentration on adsorption during continuous-flow operation. The adsorption breakthrough curve shifted towards the origin when the phenol feed concentration was increased. For initial phenol concentrations of 40 and 250 mg L^{-1}, the breakpoint was found to be 126 and 18 min, respectively, and the saturation point was 516 and 324 min. A decrease in the breakpoint and the saturation time at high initial phenol concentrations could be due to the rapid exhaustion of adsorption sites and a shorter mass transfer zone compared with a low initial phenol concentration. Based on the breakpoint

and the saturation time, the mass transfer zone was reduced by approximately 27% when the initial phenol concentration decreased by a factor of 6.25.

3.6.4. Effect of BHAC dosage

Fig. 8(c) shows the breakthrough curve of phenol adsorption onto BHAC obtained at 2 and 5 g BHAC L^{-1} at an air flow rate of 10 L min^{-1}. The time needed to reach the breakpoint increased from 36 to 90 min when the BHAC dosage increased from 2 to 5 g L^{-1}. This finding can be explained by the fact that a higher dose of BHAC creates a greater contact surface area with phenol molecules, increasing the quantity of adsorbate removed from the solution. Consistent findings were reported by Filipkowska and Waraksa [45], who demonstrated that in an airlift reactor under dynamic conditions, the adsorption capacity of chitosan depends on the adsorbent dosage.

3.6.5. Effect of phenol inlet flow rate

The breakthrough curves of the phenol inlet flow rate at 2 and 3 L h^{-1} are shown in Fig. 8(d). As can be observed, the time required to reach saturation increased from 342 to 468 min, when the flow rate decreased because a low rate of influent phenol molecules had more time to contact the BHAC. Filipskowska and Waraksa [45], based on the investigation of the adsorption of reactive dye onto chitosan in an airlift reactor, also reported that the inlet flow rate affected the accumulated adsorption capacity. Additionally, an increase in the inlet flow rate increased the sharpness of the breakthrough curve. According to Cooney [46], in liquid-phase adsorption where intraparticle diffusion is the rate-limiting transport process, C/C_0 gradually approaches 1.

4. Concluding remarks

The solution pH and the initial phenol concentration play very important roles in the adsorption of phenol onto BHAC. The highest adsorption capacity of phenol onto BHAC was achieved at pH 7, and it decreased as the pH value increased to 11, due to an electrostatic repulsion between the phenolate and ionised groups on the BHAC. The maximum adsorption capacity of phenol onto BHAC (98.83 mg g^{-1}) was similar to the values reported for commercial and lignocellulosic-based activated carbon. An adsorption equilibrium was reached within 40 and 200 min at an initial phenol concentration of 1,000 mg L^{-1} at 35˚C and 30˚C, respectively.

Desorption studies have demonstrated that the phenol-loaded BHAC can be regenerated using 10% V/V ethanol/water solutions as eluent; this adsorbent can be used for up to five adsorption/desorption cycles. The adsorption capacity of phenol onto BHAC decreased by approximately 30% from the first to the fifth cycle.

The adsorption of phenol onto BHAC from aqueous solutions was investigated at 30˚C in a continuous airlift reactor. As the air flow rate or the BHAC dosage increased, the time to achieve the breakthrough point increased as a result of more turbulent flows or more available surface area, respectively. In contrast, the breakthrough point decreased when the initial phenol concentration or the inlet flow rate increased because the adsorption sites were increasingly occupied by phenol molecules.

In summary, BHAC is a low-cost, alternative adsorbent that is comparable to commercial activated carbon for the treatment of phenol-containing wastewater. Additionally, a continuous operation seems feasible in airlift reactors when using the powdered activated carbon.

Acknowledgements

The authors thank the Facultad de Ciencias Químicas of the Universidad Autónoma de Nuevo León for providing infrastructure and CONACYT for a scholarship (60916) granted through the doctorate programme. The authors declare no conflicts of interest.

References

[1] N.C. Saha, F. Bhunia, A. Kaviraj, Toxicity of phenol to fish and aquatic ecosystems, Bull. Environ. Contam. Toxicol. 63 (1999) 195–202.
[2] R.M. Bruce, J. Santodonato, M.W. Neal, Summary review of the health effects associated with phenol, Toxicol. Ind. Health 3 (1987) 535–568.
[3] G. Busca, S. Berardinelli, C. Resini, L. Arrighi, Technologies for the removal of phenol from fluid streams: A short review of recent developments, J. Hazard. Mater. 160 (2008) 265–288.
[4] S. Altenor, B. Carene, E. Emmanuel, J. Lambert, J.J. Ehrhardt, S. Gaspard, Adsorption studies of methylene blue and phenol onto vetiver roots activated carbon prepared by chemical activation, J. Hazard. Mater. 165 (2009) 1029–1039.
[5] L.J. Kennedy, J.J. Vijaya, K. Kayalvizhi, G. Sekaran, Adsorption of phenol from aqueous solutions using mesoporous carbon prepared by two-stage process, Chem. Eng. J. 132 (2007) 279–287.

[6] L. Khenniche, F. Benissad-Aissani, Adsorptive removal of phenol by coffee residue activated carbon and commercial activated carbon: Equilibrium, kinetics, and thermodynamics, J. Chem. Eng. Data 55 (2010) 4677–4686.
[7] A.T. Mohd Din, B.H. Hameed, A.L. Ahmad, Batch adsorption of phenol onto physiochemical-activated coconut shell, J. Hazard. Mater. 161 (2009) 1522–1529.
[8] J.M.R. Rodríguez Arana, R.R. Mazzoco, Adsorption studies of methylene blue and phenol onto black stone cherries prepared by chemical activation, J. Hazard. Mater. 180 (2010) 656–661.
[9] R. Shawabkeh, E. Abu-Nameh, Absorption of phenol and methylene blue by activated carbon from pecan shells, Colloid J. 69 (2007) 355–359.
[10] V. Srihari, A. Das, The kinetic and thermodynamic studies of phenol-sorption onto three agro-based carbons, Desalination 225 (2008) 220–234.
[11] V.L. Snoeyink, W.J. Weber, H.B. Mark, Sorption of phenol and nitrophenol by active carbon, Environ. Sci. Technol. 3 (1969) 918–926.
[12] J.M.V. Nabais, J.A. Gomes, Suhas, P.J.M. Carrott, C. Laginhas, S. Roman, Phenol removal onto novel activated carbons made from lignocellulosic precursors: Influence of surface properties, J. Hazard. Mater. 167 (2009) 904–910.
[13] The National Institute of Statistics and Geography (INEGI), Estadisticas historicas de Mexico (Historical Statistics of Mexico 2009), Memoria Collection, INEGI, Mexico City, 2010.
[14] M. Loredo-Cancino, E. Soto-Regalado, F.J. Cerino-Córdova, R.B. García-Reyes, A.M. García-León, M.T. Garza-González, Determining optimal conditions to produce activated carbon from barley husks using single or dual optimization, J. Environ. Manage. 125 (2013) 117–125.
[15] C.C. Leng, N.G. Pinto, An investigation of the mechanisms of chemical regeneration of activated carbon, Ind. Eng. Chem. Res. 35 (1996) 2024–2031.
[16] D.O. Cooney, A. Nagerl, A.L. Hines, Solvent regeneration of activated carbon, Water Res. 17 (1983) 403–410.
[17] K. Mohanty, D. Das, M.N. Biswas, Treatment of phenolic wastewater in a novel multi-stage external loop airlift reactor using activated carbon, Sep. Purif. Technol. 58 (2008) 311–319.
[18] Y. Al-Degs, M.A.M. Khraisheh, S.J. Allen, M.N. Ahmad, Effect of carbon surface chemistry on the removal of reactive dyes from textile effluent, Water Res. 34 (2000) 927–935.
[19] N.E. Dávila-Guzmán, F.J. Cerino-Córdova, E. Soto-Regalado, J.R. Rangel-Mendez, P.E. Díaz-Flores, M.T. Garza-Gonzalez, J.A. Loredo-Medrano, Copper biosorption by spent coffee ground: Equilibrium, kinetics, and mechanism, Clean 41 (2013) 557–564.
[20] R.B. Garcia-Reyes, J.R. Rangel-Mendez, Adsorption kinetics of chromium(III) ions on agro-waste materials, Bioresour. Technol. 101 (2010) 8099–8108.
[21] J.S. Mattson, H.B. Mark, M.D. Malbin, W.J. Weber, J.C. Crittenden, Surface chemistry of active carbon: Specific adsorption of phenols, J. Colloid Interface Sci. 31 (1969) 116–130.
[22] I. Langmuir, The adsorption of gases on plane surfaces of glass, mica and platinum, J. Am. Chem. Soc. 40 (1918) 1361–1403.
[23] H. Freundlich, Über die adsorption in Lösungen (adsorption in Solution), Wilhelm Engelmann, Leipzig, 1906.
[24] R. Sips, On the structure of a catalyst surface, J. Chem. Phys. 16 (1948) 490–495.
[25] D.O. Cooney, adsorption design for wastewater treatment, Lewis Publishers, Washington, DC, 1998, pp. 27–36.
[26] W. Rudzinski, W. Plazinski, Studies of the kinetics of solute adsorption at solid/solution interfaces: On the possibility of distinguishing between the diffusional and the surface reaction kinetic models by studying the pseudo-first-order kinetics, J. Phys. Chem. 111 (2007) 15100–15110.
[27] R.W. Coughlin, F.S. Ezra, Role of surface acidity in the adsorption of organic pollutants on the surface of carbon, Environ. Sci. Technol. 2 (1968) 291–297.
[28] H.A. Arafat, M. Franz, N.G. Pinto, Effect of salt on the mechanism of adsorption of aromatics on activated carbon, Langmuir 15 (1999) 5997–6003.
[29] M. Franz, H.A. Arafat, N.G. Pinto, Effect of chemical surface heterogeneity on the adsorption mechanism of dissolved aromatics on activated carbon, Carbon 38 (2000) 1807–1819.
[30] O.P. Mahajan, C. Moreno-castilla, P.L. Walker, Surface-treated activated carbon for removal of phenol from water, Sep. Sci. Technol. 15 (1980) 1733–1752.
[31] E.A. Müller, K.E. Gubbins, Molecular simulation study of hydrophilic and hydrophobic behavior of activated carbon surfaces, Carbon 36 (1998) 1433–1438.
[32] S.Y. Lagergren, Zur theorie der sogenannten adsorption gelöster stoffe (About the Theory of So-called Adsorption of Soluble Substances), Kungliga Svenska Vetenskapsakad (Royal Swedish Academy of Sciences), Stockholm, 1898, pp. 1–39.
[33] Y.S. Ho, G. McKay, The sorption of lead(II) ions on peat, Water Res. 33 (1999) 578–584.
[34] W.J. Weber, J.C. Morris, Kinetics of adsorption on carbon from solution, J. Sanitary Eng. Div. 89 (1963) 31–60.
[35] T. Vermeulen, Theory for irreversible and constant-pattern solid diffusion, Ind. Eng. Chem. 45 (1953) 1664–1670.
[36] K.G. Bhattacharyya, A. Sharma, Kinetics and thermodynamics of Methylene Blue adsorption on Neem (*Azadirachta indica*) leaf powder, Dyes Pigm. 65 (2005) 51–59.
[37] M.Y. Chang, R.S. Juang, Adsorption of tannic acid, humic acid, and dyes from water using the composite of chitosan and activated clay, J. Colloid Interface Sci. 278 (2004) 18–25.
[38] Y.A. Alhamed, Adsorption kinetics and performance of packed bed adsorber for phenol removal using activated carbon from dates' stones, J. Hazard. Mater. 170 (2009) 763–770.
[39] H. Qiu, L. Lv, B.C. Pan, Q.J. Zhang, W.M. Zhang, Q.X. Zhang, Critical review in adsorption kinetic models, J. Zhejiang Univ. Science A 10 (2009) 716–724.
[40] W.H. Cheung, Y.S. Szeto, G. McKay, Intraparticle diffusion processes during acid dye adsorption onto chitosan, Bioresour. Technol. 98 (2007) 2897–2904.
[41] D.M. Ruthven, Principles of adsorption and adsorption processes, Wiley-Interscience, New York, NY, 1984, pp. 29–30.

[42] J.C. Crittenden, R.R. Trussell, D.W. Hand, K.J. Howe, G. Tchobanoglous, Adsorption, in MWH's Water Treatment, Wiley, Hoboken, NJ, 2012, pp. 1117–1262.
[43] D.W. Green, R.H. Perry, Perry's Chemical Engineers' Handbook, eighth ed., McGraw-Hill, New York, NY, 2008, pp. 43–76.
[44] US Environmental Protection Agency (USEPA), Toxicological Review of Phenol EPA/635/R-02/006, USEPA, Washington, DC, 2002.
[45] U. Filipkowska, K. Waraksa, Adsorption of reactive dye on chitosan in air-lift reactor, Adsorption 14 (2008) 815–821.
[46] D.O. Cooney, The importance of axial dispersion in liquid-phase fixed-bed adsorption operations, Chem. Eng. Commun. 110 (1991) 217–231.
[47] V. Fierro, V. Torné-Fernández, D. Montané, A. Celzard, Adsorption of phenol onto activated carbons having different textural and surface properties, Micropor. Mesopor. Mater. 111 (2008) 276–284.